p-ISSN 2301–4156 | e-ISSN 2460–5719

Subarray 4x4 for 5G MIMO Antenna with Elements that Implement Parasitic Techniques

Fitri Amillia[1,4], Eko Setijadi[2], Gamantyo Hendrantoro[3]

[1,2,3] Department of Electrical Engineering, Faculty of Intelligent Electrical and Informatics Technology, Institut Teknologi Sepuluh Nopember (ITS), Kampus ITS, Keputih, Surabaya 60111 (tel.: 031-594 7302; fax: 031-593 1237; email: [1]07111860010009@mhs.its.ac.id, [2]ekoset@ee.its.ac.id, [3]gamantyo@ee.its.ac.id)

[4] Department of Electrical Engineering, Faculty of Science and Technology, Universitas Islam Negeri Sultan Syarif Kasim Riau, Jl. H.R. Soebrantas No. 1551 KM.15 Simpang Baru Panam Pekanbaru 28293 (tel.: 0761-562051; fax: 0761-562052; email: [4]fitriamillia@uin-suska.ac.id)

[Received: 10 October 2022, Revised: 26 December 2022]
Corresponding Author: Eko Setijadi

ABSTRACT — Multiple-input multiple-output (MIMO) is a wireless communication system using multiple antennas on the transmitting and receiving sides. This system can improve the quality of wireless communication on 5G technology networks. The advantages of 5G include higher data rates and lower delays. The 5G network in Indonesia uses an intermediate frequency working in the 3.5 GHz frequency band. Antenna is an important device in a wireless network MIMO system. Therefore, this study proposes a single element design using parasitic techniques to widen the bandwidth to meet the needs of MIMO antennas and design a 4×4 subarray antenna for 5G MIMO. The method used began with determining the target antenna specifications, then designing a single element with a parasitic patch. The use of parasitic patches techniques on antenna elements aims to widen the bandwidth to meet target specifications. The resonant frequency of the microstrip antenna was affected by the increase in the number of parasitic patches. The number of resonant frequencies that arise resulted in a broad bandwidth. Then, the single elements with parasitic patches were arranged into a 4x4 subarray. All elements were arranged on the same substrate with a spacing between elements from one feed point to another was 64.28 mm or 0.75λ. The subarray design met the target antenna specifications if the subarray elements have a fractional bandwidth of more than 20% and mutual coupling of less than -20 dB. The material used in antenna design and fabrication was FR-4 (epoxy) substrate with a dielectric constant (ε_r) of 4.3 and a substrate thickness (h) of 1.6 mm. The results showed a bandwidth of 735 MHz or a fractional bandwidth of 20.35%, return loss of -14.65 dB, mutual coupling of -30.05 dB, and gain of 16.86 dB. Thus, the designed 4x4 subarray for MIMO antenna meets the desired specifications.

KEYWORDS — MIMO, Subarray, 5G, Microstrip, Parasitic.

I. INTRODUCTION

The multiple-input multiple-output (MIMO) system is one of the main keys of 5G technology [1], [2]. MIMO technology originates from the technology diversity of wireless communication antennas and smart antennas. This system is a combination of multiple-input single-output (MISO) and single-input multiple-output (SIMO) which have the advantages and characteristics of both. The system contains several transmitters and receivers that have their own antennas [3]. Some of the advantages of this system include high data rates, reliability, and spectral efficiency [4].

The antenna is an important device in supporting the performance of the 5G wireless technology using MIMO system. One of the recommended 5G frequency allocations is the medium frequency, namely the 3.5 GHz frequency, which will be used in Indonesia due to its wide coverage thereby saving network development costs [5]. In realizing a MIMO antenna system, it is necessary to design an antenna with a wide bandwidth supporting various system services and high gain [6]. MIMO antennas are often designed using microstrip technologies due to their low cost, low profile, compactness, and ease of integration. At the same time, their disadvantages include the narrow bandwidth, small gain, and directivity [7].

Several antenna designs to increase bandwidth include the circular antenna design with the stacked patch method with an increased bandwidth of 7.3% [8]. A single antenna design combining a modified parasitic patch method with a slot patch [9] and a single element design combining the u-shaped method with a parasitic method resulted in a 10.3% increase in bandwidth [10].

Reference [11] studied the antenna design consisting of a substrate layer with four parasitic patches placed on the top layer of the antenna, while the array application was realized using a combination of two decoupling techniques by assembling a 2x2 antenna. The two techniques used were decoupling walls and neutralized networks. Metal walls not only made it easy for the two parasitic patches to short-circuit, but also acted as decoupling walls to reduce mutual coupling between antenna elements which was detrimental. Furthermore, simple decoupling with short-circuit stepped impedance structures (SSIS) as a neutralizer network was added to suppress mutual coupling. The antenna consisted of two layers of substrate with a thickness of 1.5 and 2 mm, respectively. The antenna structure was a rectangular cavity formed by metal via as sidewalls. Here, the two substrate layers were used with the SSIS decoupling technique in the array configuration. It caused the antenna to be more expensive to manufacture and less compact. This design operated in the frequency range of 3.35 to 3.95 GHz or fractional bandwidth of 16%, gain of 13.6 dB, and mutual coupling below -38 dB.

Reference [12] studied a two-element subarray design using five parasitic patches placed on the top layer of the antenna and one layer of the substrate. The design was simulated and arranged in an H-plane with a distance of 0.75λ resulting in a mutual coupling of -29.76 dB and an E-field of -33.56 dB. On the other hand, the mutual coupling in the E-plane for a distance of 0.5λ did not meet the criteria. Fractional bandwidth of 17%, with the resulting frequency range of 609.9–616.4 MHz for all variations of element spacing, was suitable for 5G applications.

Then, [6] examined the effect of parasitic patch elements on the MIMO antenna performance. Multiple rectangular patch parasitic elements were added near each rectangular patch element. These parasitic elements affected the distribution of the electromagnetic field and consequently reduced mutual coupling. In addition, wider bandwidth was also achieved. The proposed design was composed of two MIMO antennas coupled in an H-plane and an E-plane with a rated bandwidth of 14%.

This study proposes elements using the parasitic patch technique to be implemented in a 4×4 subarray design on a MIMO system antenna with a working frequency of 3.5 GHz. Furthermore, this study develops the technique of adding a parasitic patch to the top layer to produce several resonant frequencies that produce a wider bandwidth [6], [12]-[15]. The number of parasitic patches used in [6] was three parasitic patches, [12] was five parasitic patches, [13] was four parasitic patches, [14] was three parasitic patches, and [15] was three parasitic patches. Meanwhile, this study applied ten parasitic patches. According to the ETSI standard, the 5G bandwidth requirement for the 3.5 GHz frequency is a minimum of 500 MHz [16], and mutual coupling is less than -20 dB [6]. It is hoped that this study can produce bandwidth greater than 600 MHz or fractional bandwidth of around 20% and mutual coupling which is smaller than -20 dB. After obtaining the design elements according to the desired specifications, these elements were arranged into a 4×4 subarray for a MIMO antenna system with a spacing between elements based on a feeding point of 0.75λ. Furthermore, the performance evaluation of the MIMO antenna subarray was carried out with parameters including return loss, bandwidth, mutual coupling, gain, beamwidth, and sidelobe level (SLL).

This paper is divided into five sections. The first section is an introduction, the second section describes the microstrip antenna and parasitic techniques, the third section discusses antenna design, the fourth section is the results and analysis, and the final section contains the conclusions.

II. MICROSTRIP ANTENNA

A. MICROSTRIP RECTANGULAR PATCH ANTENNA

The microstrip rectangular patch antenna is the most widely used type of microstrip antenna since this type of antenna is easier to analyze. The structure of a rectangular patch microstrip antenna has a thickness (h), width (W), and stretches along (L). The structure of a microstrip antenna consists of a patch, substrate, and ground plane which can be seen in Figure 1(a).

In designing a rectangular patch microstrip antenna, the parameters that need to be known are the dimensions of length (L) and width (W). To obtain the dimensions of length (L) and width (W), (1) through (4) can be used [17], [18].

$$W = \frac{c}{2f_r}\sqrt{\frac{2}{\varepsilon_r+1}} \quad (1)$$

$$L = L_{eff} - 2\Delta L \quad (2)$$

$$L_{eff} = \frac{c}{2f_r\sqrt{\varepsilon_{reff}}} \quad (3)$$

$$\Delta L = 0.412\,h\,\frac{(\varepsilon_{reff}+0.3)+(\frac{W}{h}+0.264)}{(\varepsilon_{reff}+0.258)+(\frac{W}{h}+0.8)} \quad (4)$$

with

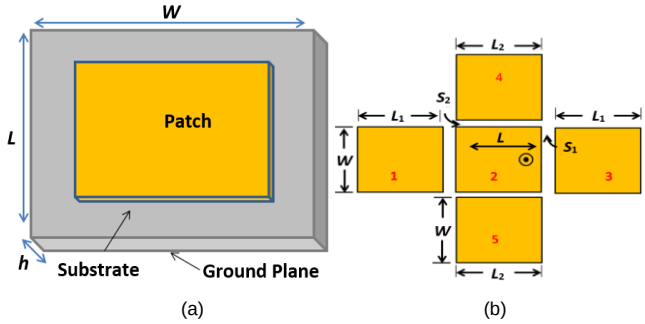

Figure 1. Microstrip antenna, (a) microstrip rectangular patch antenna, (b) configuration of antenna with four parasitic patch elements [13].

f_r = resonant frequency or antenna frequency (Hz)
c = speed of light (3.10^9 m/s)
h = substrate thickness (mm)
ε_r = dielectric constant of the substrate
L_{eff} = effective patch length (mm)
ε_{reff} = effective dielectric constant.

Meanwhile, the length and width of the ground plane can be calculated using (5) and (6) [18], [19].

$$L_g = xh + L \quad (5)$$

$$W_g = xh + W \quad (6)$$

with
L_g = ground plane length (mm)
W_g = ground plane and substrate width (mm)
x = multiplier factor with value ≥ 6.

In the coaxial probe distribution point, the antenna distribution point greatly affects the performance of the antenna. Therefore, the antenna feed point can be calculated using (7) to (9) [18], [20]:

$$\varepsilon_{reff} = \frac{(\varepsilon_r+1)}{2}+\frac{(\varepsilon_r-1)}{2}\left[1+12\frac{h}{W}\right]^{-\frac{1}{2}} \quad (7)$$

$$X_f = \frac{L}{2\sqrt{\varepsilon_{reff}}} \quad (8)$$

$$Y_f = \frac{W}{2} \quad (9)$$

with

ε_{reff} = effective dielectric constant
ε_r = dielectric constant of the substrate
h = substrate thickness (mm)
W = patch width (mm)
X_f = long side feed point (mm)
Y_f = wide edge feed point (mm).

B. PARASITIC TECHNIQUE

The parasitic patch technique was applied by adding a patch or placing the patch near the edge of the original patch antenna. This new patch, called the parasitic patch, could be connected to the main patch antenna electromagnetically. This technique is one way to increase the bandwidth of microstrip antennas [21].

Each parasitic patch could be designed in the same way as the original patch antenna. The design of the parasitic patch was based on calculations from several mathematical equations that have been mentioned in (1) to (9) and adjusted to the specifications of the material used. The length and width of the

JURNAL NASIONAL TEKNIK ELEKTRO DAN TEKNOLOGI INFORMASI
p-ISSN 2301–4156 | e-ISSN 2460–5719

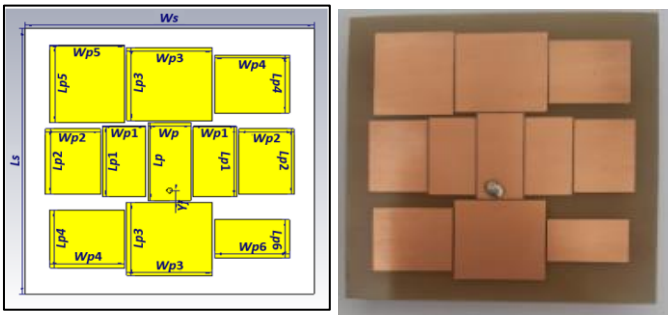

(a) (b)

Figure 2. Single element, (a) design, (b) fabrication results.

TABLE I
SINGLE ELEMENT DIMENSIONS

Symbol	Value (mm)	Symbol	Value (mm)	Symbol	Value (mm)
Ws	68.71	$Wp1$	10.31	$Wp4$	17.77
Ls	68.49	$Lp1$	18.27	$Lp4$	15.00
Wp	10.25	$Wp2$	13.13	$Wp5$	17.77
Lp	20.11	$Lp2$	16.97	$Lp5$	20.00
Xf	6.09	$Wp3$	20.39	$Wp6$	17.77
Yf	2.80	$Lp3$	18.89	$Lp6$	10.00

parasitic patch determined the resonant frequency and the resulting bandwidth [13].

The parasitic patch obtained an electric current due to the induction from the main patch. The main patch was supplied with an electric current, then the electric current that was in the main patch caused an induction on the side radiating the parasitic patch. The different dimensions of the parasitic patch affected the change in the resonant frequency. Coupling between parasitic patches was affected by the distance between the parasitic patches which could control the antenna impedance matching. After that, the parasitic patch element configurations 1, 2 and 3 were arranged horizontally as shown in Figure 1(b).

Since the distance between the parasitic patches was close to each other, the parasitic patch on the side that was not radiating generated an electric current because of induction from the parasitic patch on the side that was radiating. The electric field was not uniform on the edges that were not radiating; meanwhile, on the edges that were radiating, the electric field was uniform. Furthermore, the configuration of parasitic patch element 4, element 2, and element 5 was arranged vertically as shown in Figure 1(b).

The configuration of a microstrip antenna with four-element parasitic patch coupling combined two methods, namely coupling through the radiating edge and coupling through the nonradiating edge, so as to increase the bandwidth as shown in Figure 1(b).

III. ANTENNA DESIGN

This stage was begun with a single element design using a parasitic patch which was arranged in the form of a subarray with a 4×4 configuration for 5G MIMO system antennas. The feeding technique used in the antenna was a coaxial feeding probe.

The specifications targeted were MIMO system antennas with a working frequency of 3.5 GHz according to 5G requirements [5]; bandwidth of ≥ 600 MHz [16]; fractional bandwidth of ≥ 20%; return loss of ≤ −10 dB; mutual coupling

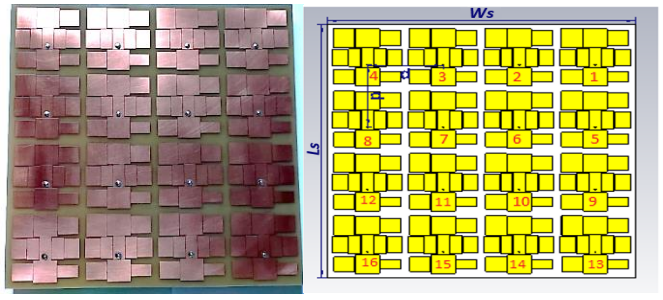

(a) (b)

Figure 3. 4×4 subarray, (a) fabrication results, (b) design.

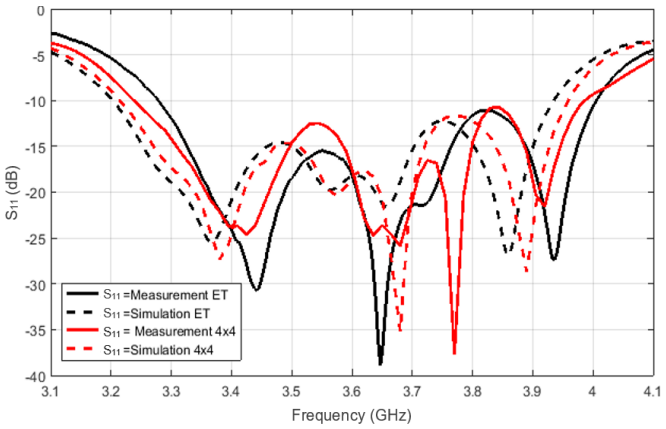

Figure 4. Simulation results and measurements of return loss and bandwidth single element and 4×4 subarray.

of ≤ −20 dB [6], [11], [12]; and gain of > 3 dB [6]. The material used in antenna design and fabrication was FR-4 (epoxy) substrate with a dielectric constant (ε_r) of 4.3 and a substrate thickness (h) of 1.6 mm.

Furthermore, in the early stages, a rectangular single-element design without a parasitic patch was in accordance with the expected specifications, namely working at a frequency of 3.5 GHz. Then, to design a single element using the parasitic patch technique to get the desired antenna performance, it is necessary to optimize the antenna design by changing the parameters of the parasitic patch to provide optimal performance. In optimizing this antenna, several changes were made to the dimensions of the parasitic patch by reducing the dimension width and adding several parasitic patches in such a way that it could reach the target specifications, including working frequency, gain, and bandwidth.

After the single element using the parasitic patch met the target, it was then arranged in a 4×4 subarray structure. The subarray design was considered to have met the target if the subarray elements already had a fractional bandwidth of more than 20% and the antenna parameter criteria had also been met. The subarray antenna was arranged using a 4×4 planar configuration. All elements were arranged on the same substrate with spacing between elements from one feeder point to another of 64.28 mm or 0.75λ. The distance between these elements had met the target, which was to produce less than mutual coupling of −20 dB.

The design was carried out to manufacture the antenna realization after the single element design and 4×4 subarray was in accordance with the target antenna specifications. Furthermore, the antenna realization for a single element was

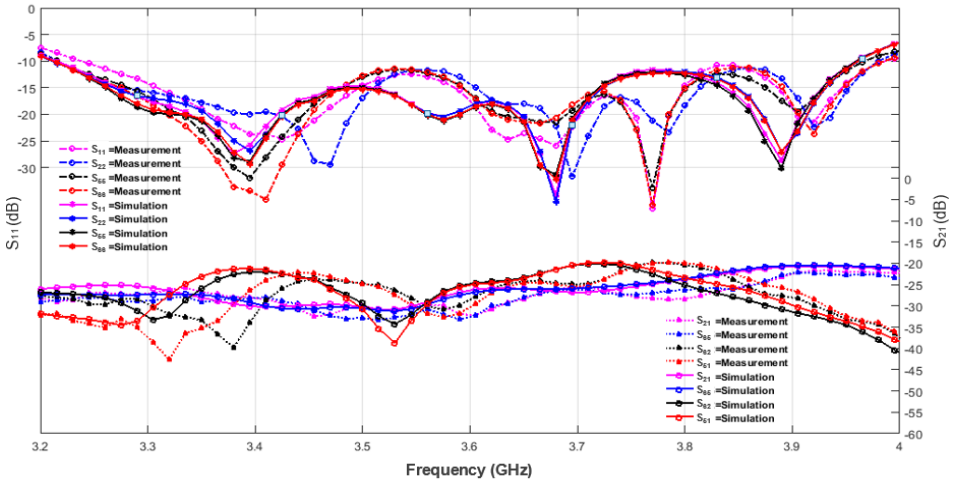

Figure 5. Simulation and measurement results of single element s-parameters and 4×4 subarray.

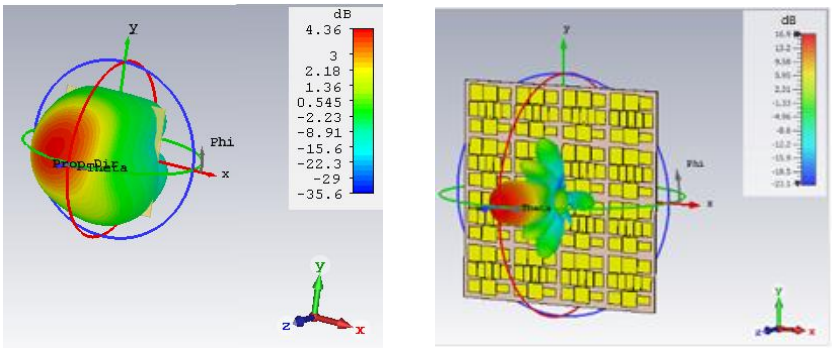

(a) (b)

Figure 6. Gain, (a) single element and (b) 4×4 subarray.

simulated and measured in the anechoic chamber, whereas the 4×4 subarray was only simulated.

A. SINGLE ELEMENT DESIGN

In this stage, a single element was created by combining ten parasitic patches operating in 3.5 GHz. The use of a parasitic patch technique on a single element was intended to widen the bandwidth. The addition of the parasitic patch [13] caused several changes were made to the parasitic patch, especially in the Wp and Lp dimensions, $Wp1$ and Lp dimensions, $Wp2$ and $Lp2$ dimensions, $Wp3$ and $Lp3$ dimensions, as well as the addition of parasitic patches with $Wp4$ and Lp dimensions, $Wp5$ and $Lp5$ dimensions, $Wp6$ and $Lp6$ dimensions is shown in Figure 2(a). The length and width of the parasitic patch and the placement of the parasitic patch horizontally (H-field) and vertically (E-field) determine the new resonance frequency, which can increase the bandwidth [6], [12]–[15]. The position of the parasitic patch with $Wp4$ and $Lp4$ dimensions, $Wp5$ and $Lp5$ dimensions, $Wp6$ and $Lp6$ dimensions is shown in Figure 2(a). The parasitic patch gets an electric current due to the induction of the parasitic patch with Wp and Lp dimensions. At first Wp and Lp, dimension patches were supplied with an electric current. Then, the electric current in the Wp and Lp, dimension parasitic patches caused induction on the radiating side of the parasitic patch. Since the distance between the parasitic patches was close to each other, an electric current arose in the parasitic patch on the side that was not radiating due to the induction of the parasitic patch on the side that was radiating.

The addition of a parasitic patch was done to obtain dimensions with width and length that need to be optimized so as to provide more optimal performance according to the expected antenna specifications. The design dimensions of a single element with ten parasitic patches were generated from mathematical calculations following (1) to (9) based on [17], [18]. The dimensions are shown in Table I and the design in geometric form can be seen in Figure 2(a). After obtaining the appropriate dimensions and designs as shown in Figure 2(a), then a 4×4 subarray was arranged, as shown in Figure 3.

B. 4×4 SUBARRAY DESIGN

After a single element design that meets the specifications was obtained, it was then arranged into a 4×4 subarray configuration. The subarray consisted of sixteen elements. The spacings between adjacent elements based on the location of the feed points were 0.75λ or 64.28 mm, respectively. The width of the space between the elements was determined based on the dimensions of the elements which were quite large after the addition of ten parasitic patches. On the other hand, the wide enough spacing was expected to be able to suppress the mutual coupling effect. The subarray design met antenna specifications if the subarray elements already had a fractional bandwidth of more than 20% and mutual coupling of less than -20 dB. Furthermore, the resulting subarray design dimensions were Ws = 261.55 mm, Ls = 261.33 mm. The geometry can be seen in Figure 3(a).

IV. RESULT AND ANALYSIS

At this stage, the simulation results were compared to measurements. The simulation used computer simulation technology (CST), which was software for the antenna simulation to design single elements and 4×4 subarrays.

p-ISSN 2301–4156 | e-ISSN 2460–5719

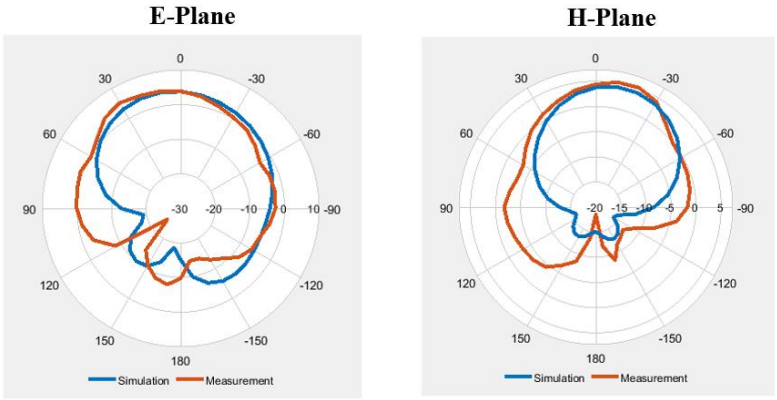

(a) (b)

Figure 7. Comparison of simulation and measurement of single element radiation patterns, (a) E-plane, (b) H-plane.

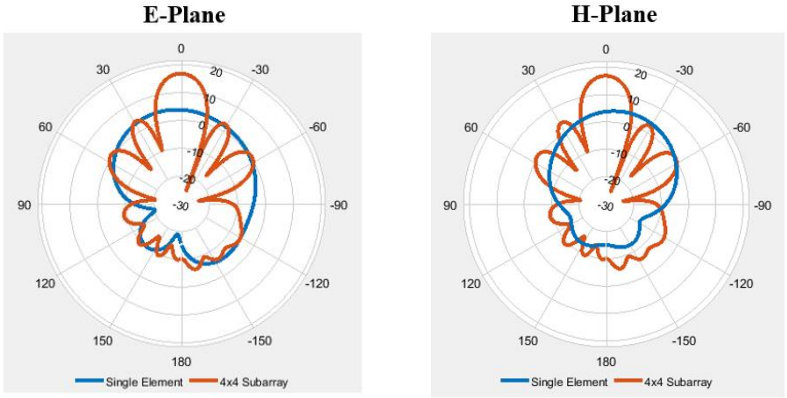

(a) (b)

Figure 8. Comparison of single element radiation pattern simulation and 4x4 Subarray, (a) E-plane, (b) H-plane.

Antenna performance parameters observed included return loss (S_{11}), bandwidth, mutual coupling (S_{21}), SLL, and gain.

A. S-PARAMETER PERFORMANCE

The single element fabrication results are shown in Figure 2(b) and the 4×4 subarray is shown in Figure 3(b). The simulation results and measurements of return loss and bandwidth of the single element design and 4×4 subarray at 3.5 GHz are shown in Figure 4.

The single element simulation results for the return loss parameter (S_{11}) were -14.99 dB. Antenna bandwidth could be calculated from the value of return loss below -10 dB. Bandwidth was 732 MHz and fractional bandwidth was 20.52%. Meanwhile, the measurement results for the return loss parameter (S_{11}) were -18.42 dB, a bandwidth of 722 MHz, and a fractional bandwidth of 19.83%.

Then, the simulation results for the 4×4 subarray design for the return loss parameter (S_{11}) were -14.65 dB. The resulting bandwidth was 733 MHz with a fractional bandwidth of 20.49%. As a comparison, the measurement results for the 4×4 subarray design for the return loss parameter (S_{11}) was -14.59 dB, the bandwidth was 735 MHz, and the fractional bandwidth was 20.35%.

Next, Figure 5 shows a comparison of the simulation results and measurements of the S-parameter return loss and mutual coupling for the 4×4 subarray design at 3.5 GHz. Since the elements in the subarray formed a symmetry as shown in Figure 5, the results reported to represent the 4×4 subarray were the 1, 2, 5, and 6 elements.

The return loss simulation results (S_{11}) were -14.65 dB, S_{22} was -15.10 dB, S_{55} was -14.97 dB, S_{66} was -15.19 dB. The results of the mutual coupling simulation (S_{21}) were -30.23 dB, S_{65} was -30.62 dB, S_{62} was -29.41 dB, and S_{51} was -30.71 dB. The measurement results for S_{21} was -30.05 dB, S_{65} was -32.81 dB, S_{62} was -24.76 dB, and S_{51} was -24.81 dB. Elements 3, 7, 9, and 10 in the 4×4 subarray in Figure 3(a) formed a symmetry with other elements for mutual coupling with adjacent elements such as S_{67} similar to S_{21}, S_{65}, for S_{610} similar to S_{62} , S_{51}, for S_{23} similar to S_{21}, S_{65}, for S_{59} similar to S_{62}, S_{51}.

B. RADIATION PATTERN PERFORMANCE

The simulation results of the 3D far-field radiation pattern and gain are shown in Figure 6(a) for a single element antenna and Figure 6(b) for a 4×4 subarray. The strength of the gain parameter value is shown by color degradation. The degradation of the color from blue shows the lowest gain, while the degradation of the red color shows the highest gain. The gain for a single element antenna was 4.36 dB. On the other hand, the gain for the 4×4 subarray was 16.86 dB.

Figure 7 shows a single element radiation pattern at a frequency of 3.5 GHz which is directional. In the E-plane with phi = 90º, it had a main lobe magnitude of 4 dB, main lobe direction of 10º, angular beamwidth (3dB) of 87°, and SLL of -9.3 dB. The H-plane was phi 0º field, generating a main lobe magnitude of 4.27 dB, main lobe direction of 140, angular beamwidth (3dB) of 70.6°, and SLL of -17.0 dB.

Comparison of single element radiation patterns between the simulation results and measurements can be seen in Figure 7. The simulation resulted in a gain of 4.36 dB, which was smaller than the measurement producing a gain of 5.34 dB. The single element antenna gains already exceeded the targeted antenna design specifications.

TABLE II
SIMULATION AND MEASUREMENT PERFORMANCE RESULTS OF SINGLE ELEMENT AND 4X4 SUBARRAY

Performance Parameters	Single Element		4x4 Subarray	
	Sim.	Meas.	Sim.	Meas.
Return loss (dB)	-14.99	-18.42	-14.65	-14.59
Bandwidth (MHz)	732	722	733	735
Fractional BW (%)	20.52	19.83	20.49	20.35
Mutual coupling (dB)	N/A	N/A	-30,23	-30.05
Gain (dB)	4.36	5.34	16.86	-

Figure 8 shows the radiation pattern of a polar 4×4 subarray. The results of the E-plane were phi 90° radiation pattern, that had a main lobe magnitude of 16.9 dB, an angular beamwidth (3dB) of 17.2°, and an SLL of -12.9 dB. The results of the H-plane were phi 0° radiation pattern, producing a main lobe magnitude of 16.9 dB, an angular beamwidth (3dB) of 17.3°, and an SLL of -12.7 dB. Comparison of simulated radiation patterns of single elements and 4×4 subarrays in Figure 8 shows the increased gain on the 4×4 subarray.

All simulation results and performance measurements of S-parameters and radiation patterns are tabulated in Table II. In Table II, "Sim." denotes Simulation and "Meas." denotes Measurement. The measurement results for the 4×4 subarray showed that the bandwidth was 13 MHz wider, and the fractional bandwidth increased by 0.52% with a gain of 12.5 dB, which was higher than that of a single element.

The 4×4 subarray showed a smaller return loss value but still meets the target antenna specifications. Then, the mutual coupling of the 4×4 subarray, which was -30.05 dB, was smaller than -20 dB, so that it was in accordance with the expected target and there was no need for other methods to reduce mutual coupling. Therefore, single element and 4×4 subarrays produced a bandwidth of up to 700 MHz or a fractional bandwidth increase of up to 20%, so that they met the desired target antenna specifications.

V. CONCLUSION

The design of a 4×4 subarray consisting of elements using parasitic techniques for 5G MIMO antennas working at a frequency of 3.5 GHz has been carried out and tested by simulation and measurement. Each antenna element had a rectangular patch plus ten parasitic patches. These elements were then arranged into a 4×4 subarray. The addition of parasitic patches on each element is expected to increase bandwidth as well as increase the dimensions and spacing of elements so that mutual coupling is no longer a problem. Based on the simulation and measurement results, the antenna design met the desired target specifications, including increased bandwidth of up to 20.35%, gain of 16.86 dB, and mutual coupling of -30.05 dB. Hence, all parameter performance increases after being compiled into 4×4 subarrays.

CONFLICT OF INTEREST

The author declares that there is no conflict of interest in the research and writing of this article.

AUTHOR CONTRIBUTION

Conceptualization, Fitri Amillia, Eko Setijadi and Gamantyo Hendrantoro; methodology, Fitri Amillia; writing—preparation of the original draft, Fitri Amillia, Eko Setijadi and Gamantyo Hendrantoro; writing—reviewing and editing, Eko Setijadi and Gamantyo Hendrantoro; supervision, Eko Setijadi; corresponding author.

ACKNOWLEDGMENT

Fitri Amillia's doctoral studies were funded by the Ministry of Religion of the Republic of Indonesia through the Ministry of Religions Affairs (MORA) 5000 Doctoral Program number 2644/DJ.I/Dt.I.III/PP.04/08/2018. Research funded by the Ministry of Research, Technology, and Higher Education of the Republic of Indonesia through the research grant of Konsorsium Riset Unggulan Perguruan Tinggi (KRUPT) Number 705/PK S/ITS/2019.

REFERENCES

[1] D. BORGES, P. Montezuma, R. Dinis, and M. Beko, "Massive Mimo Techniques for 5G and Beyond—Opportunities and Challenges," *Electron.*, Vol. 10, No. 14, pp. 1–29, Jul. 2021, doi: 10.3390/electronics10141667.

[2] K. Jones A.S., L. Olivia N., and B. Syihabuddin, "Perancangan Antena MIMO 2×2 Array Rectangular Patch dengan U-Slot untuk Aplikasi 5G," *J. Nas. Tek. Elektro, Teknol. Inf.*, Vol. 6, No. 1, 2017, doi: 10.22146/jnteti.v6i1.299.

[3] Q. Wang *et al.*, "5G MIMO Conformal Microstrip Antenna Design," *Wirel. Commun., Mob. Comput.*, Vol. 2017, pp. 1–11, Dec. 2017, doi: 10.1155/2017/7616825.

[4] N.L. Nguyen, "Gain Enhancement in MIMO Antennas Using Defected Ground Structure," *Prog. Electromagn. Res. M*, Vol. 87, pp. 127–136, 2019, doi: 10.2528/pierm19091102.

[5] Tim Peneliti Puslitbang SDPPI, *Studi Lanjutan 5G Indonesia 2018 Spektrum Outlook dan Use Case untuk Layanan 5G Indonesia*, E.A. Maranny, H.R. Sekar H., and A. Anggorosesar, Eds., Jakarta, Indonesia: Puslitbang Sumber Daya, Perangkat, dan Penyelenggaraan Pos dan Informatika, Badan Penelitian dan Pengembangan Sumber Daya Manusia, Kementerian Komunikasi dan Informatika, 2018.

[6] H.H. Tran and N. Nguyen-Trong, "Performance Enhancement of MIMO Patch Antenna Using Parasitic Elements," *IEEE Access*, Vol. 9, pp. 30011–30016, 2021, doi: 10.1109/ACCESS.2021.3058340.

[7] G.A.T. Stutzman and Warren L., *Antenna Theory and Design*, 3rd ed., West Virginia, USA: John Wiley & Sons, Inc., 2012..

[8] Y. Wen *et al.*, "Bandwidth Enhancement of Low-Profile Microstrip Antenna for MIMO Applications," *IEEE Trans. Antennas, Propag.*, Vol. 66, No. 3, pp. 1064–1075, Mar. 2018, doi: 10.1109/TAP.2017.2787542.

[9] M.H. Reddy *et al.*, "Bandwidth Enhancement of Microstrip Patch Antenna using Parasitic Patch," in *Int. Conf. Smart Techn., Manag. Comput. Commun. Controls Energy Materials (ICSTM)*, 2017, pp. 295–298, doi: 10.1109/ICSTM.2017.8089172.

[10] X.P. Chen, N.W. Liu, and A.G. Fu, "A Compact Wideband Microstrip-Fed Patch Antenna Using a U-Shaped Parasitic Element," *2019 IEEE Int. Conf. Comput. Electromagn. (ICCEM)*, 2019, pp. 1–3, doi: 10.1109/COMPEM.2019.8779079.

[11] K.D. Xu, J. Zhu, S. Liao, and Q. Xue, "Wideband Patch Antenna Using Multiple Parasitic Patches and Its Array Application with Mutual Coupling Reduction," *IEEE Access*, Vol. 6, pp. 42497–42506, Jul. 2018, doi: 10.1109/ACCESS.2018.2860594.

[12] A.R. Pratiwi, E. Setijadi, and G. Hendrantoro, "Design of Two-Elements Subarray with Parasitic Patch for 5G Application," *2020 Int. Semin. Intell. Technol., Its Appl. (ISITIA)*, 2020, pp. 311–316, doi: 10.1109/ISITIA49792.2020.9163785.

[13] S.A.R. Parizi, "Bandwidth Enhancement Techniques," in *Microstrip Antennas Trends in Research on Antennas*, S. Chattopadhyay, Ed. London, United Kingdom: IntechOpen, 2017, doi: 10.5772/intechopen.70173, access date: 20-Sep-2022.

[14] K. Ding *et al.*, "A Compact Printed Unidirectional Broadband Antenna with Parasitic Patch," *IEEE Antennas Wirel. Propag. Lett.*, Vol. 16, pp. 2341–2344, Jun. 2017, doi: 10.1109/LAWP.2017.2718000.

[15] K.D. Xu *et al.*, "Microstrip Patch Antennas with Multiple Parasitic Patches and Shorting Vias for Bandwidth Enhancement," *IEEE Access*, Vol. 6, pp. 11624–11633, 2018, doi: 10.1109/ACCESS.2018.2794962.

[16] (2018) "ETSI Deliverable Status," [Online], https://portal.etsi.org/TB/ETSI-Deliverable-Status, access date: 28-Oct-2022.

p-ISSN 2301–4156 | e-ISSN 2460–5719

[17] S.K. Jose and S. Suganthi, "Rectangular Microstrip Antenna for WLAN Application," *2015 Int. Conf. Innov. Information, Embed., Commun. Syst.*, 2015, pp. 1–5, doi: 10.1109/ICIIECS.2015.7192986.

[18] C.A. Balanis, *Antenna Theory: Analysis and Design*, 4th ed., Hoboken, New Jersey:John Wiley & Sons, Inc., 2016.

[19] T.J. Salai Thillai and T.R. Ganesh Babu, "Rectangular Microstrip Patch Antenna at ISM Band," *2018 Second Int. Conf. Comput. Methodol., Commun. (ICCMC)*, 2018, pp. 91–95, doi: 10.1109/ICCMC.2018.8487877.

[20] A. Majumder, "Rectangular Microstrip Patch Antenna Using Coaxial Probe Feeding Technique to Operate in S-Band," *Int. J. Eng. Trends Technol.*, Vol. 4, No. 4, pp. 1206–1210, Apr. 2013.

[21] G. Kumar and K.P. Ray, *Broadband Microstrip Antenna*. Massachusetts, USA: Artech House Inc., 2003.